DOI: 10.1534/genetics.108.088591

Relationship of *Pax6* Activity Levels to the Extent of Eye Development in the Mouse, *Mus musculus*

Jack Favor,*,[1] Christian Johannes Gloeckner,* Angelika Neuhäuser-Klaus,* Walter Pretsch,* Rodica Sandulache,* Simon Saule[†] and Irmgard Zaus*

**Institute of Human Genetics, Helmholtz Zentrum München, German Research Center for Environmental Health, D-85764 Neuherberg, Germany and* [†]*Centre National de la Recherche Scientifique, UMR 146, Institut Curie Section de Recherche, Centre Universitaire, 91405 Orsay Cedex, France*

Manuscript received March 6, 2008
Accepted for publication April 28, 2008

ABSTRACT

In this study we extend the mouse *Pax6* mutant allelic series to include a homozygous and hemizygous viable hypomorph allele. The *Pax6*$^{132\text{-}14Neu}$ allele is a Phe272Ile missense mutation within the third helix of the homeodomain. The mutant *Pax6* homeodomain shows greatly reduced binding activity to the P3 DNA binding target. Glucagon-promoter activation by the entire mutant *Pax6* product of a reporter gene driven by the G1 paired and homeodomain DNA binding target was slightly increased. We constructed mutant *Pax6* genotypes such that *Pax6* activity ranged between 100 and 0% and show that the extent of eye development is progressively reduced as *Pax6* activity decreased. Two apparent thresholds identify three groups in which the extent of eye development abruptly shifted from complete eye at the highest levels of *Pax6* to a rudimentary eye at intermediate levels of *Pax6* to very early termination of eye development at the lowest levels of *Pax6*. Of the two *Pax6*-positive regions that participate in eye development, the surface ectoderm, which develops into the lens vesicle and the cornea, is more sensitive to reduced levels of *Pax6* activity than the optic vesicle, which develops into the inner and outer retinal layers.

THE transcription factor *Pax6* belongs to the family of paired-box-containing genes and is highly conserved over a wide range of phyla within the kingdom animalia. The mouse *Pax6* gene encodes a protein with DNA binding paired and homeodomains separated by a linker region, and a C-terminal proline-, serine-, and threonine-rich transcriptional activation domain (Walther and Gruss 1991; Glaser *et al.* 1994). By mutant analysis *Pax6* was shown to function in the development of the eye (Theiler *et al.* 1978; Hogan *et al.* 1986, 1988; Hill *et al.* 1991; Baulmann *et al.* 2002), olfactory tissues (Hogan *et al.* 1986; Heinzmann *et al.* 1991; Grindley *et al.* 1995; Quinn *et al.* 1996), craniofacial traits (Kaufman *et al.* 1995), the central nervous system (Schmahl *et al.* 1993; Stoykova *et al.* 1996, 1997, 2000; Grindley *et al.* 1997; Götz *et al.* 1998), the pancreas (St-Onge *et al.* 1997), the pituitary gland (Bentley *et al.* 1999; Kioussi *et al.* 1999), the pineal gland (Estivill-Torrús *et al.* 2001) and adult neurogenesis (Hack *et al.* 2005). For correct development of the eye a critical range of *Pax6* expression is required since heterozygous carriers of *Pax6* deletions (Hogan *et al.* 1986; Ton *et al.* 1991) and transgenic mice with increased levels of *Pax6* (Schedl *et al.* 1996) both express eye abnormalities.

Pax6 gene products control the transcriptional activity of target genes by directly or indirectly (via oligomerization with additional cofactors) binding to enhancer DNA target sequences (Chi and Epstein 2002). The "level" of *Pax6* gene activity cannot be considered the sum of activities of the individual domains since missense mutations confined to a single domain can affect the binding activity of the full-length gene product by the second nonmutated domain and can alter the spectrum of gene target sequences to which the mutated gene product binds (Tang *et al.* 1997; Singh *et al.* 2000; Mishra *et al.* 2002). Similarly, missense mutations in the C-terminal proline-, serine-, and threonine-rich transcription activation domain can affect the DNA binding activity of the gene product by the paired or homeodomains (Singh *et al.* 2001). The situation is further complicated since *Pax6* is expressed as a number of isoforms (Carrière *et al.* 1993, 1995; Wawersik *et al.* 2000; Gorlov and Saunders 2002). Thus, although DNA binding activity of isolated *Pax6* domains to specific DNA target sequences or reporter gene activation by specific *Pax6* isoforms can be measured, such results do not reflect the *in vivo* situation of a mixture of multiple isoforms simultaneously binding to a range of alternate target sites. Previous experimental approaches to address the question of the consequences of altering

[1]*Corresponding author:* Institute of Human Genetics, Helmholtz Zentrum München, German Research Center for Environmental Health, Ingolstaedter Landstrasse 1, D-85764 Neuherberg, Germany. E-mail: favor@helmholtz-muenchen.de

the levels of *Pax6* on developmental outcome have included the use of mouse null mutations (Van Raamsdonk and Tilghman 2000), $Pax6^{-/-} \leftrightarrow Pax6^{+/+}$ chimera (Quinn *et al.* 1996; Collinson *et al.* 2000, 2001, 2003; Talamillo *et al.* 2003), conditional inactivation of *Pax6* in a tissue- and stage-specific manner (Ashery-Padan *et al.* 2000; Davis-Silberman *et al.* 2005), overexpression of *Pax6* via transgenic mutant constructs (Schedl *et al.* 1996; Duncan *et al.* 2000; Kim and Lauderdale 2006, 2008; Manuel *et al.* 2007) and retrovirally mediated *Pax6* expression (Heins *et al.* 2002; Hack *et al.* 2005). We have taken a genetic approach utilizing members of the mouse *Pax6* allelic series. We identified and characterized the first homozygous viable *Pax6* hypomorph allele. With this extension of the *Pax6* allelic series we constructed *Pax6* mutant genotypes such that the predicted Pax6 activity ranged from 100% normal to 0% and assessed the extent of eye development.

MATERIALS AND METHODS

Mice, mapping, and slit lamp examination: The original mutant, designated 132, was recovered as a heterozygote expressing anterior pyramidal opacity with corneal adhesions in the offspring of a $(102/El \times C3H/El)F_1$ male exposed to 4.55 + 4.55 Gy γ-irradiation and mated to an Oak Ridge tester-stock female. Confirmation crosses indicated the mutation to be autosomal dominant (Kratochvilova and Ehling 1979). Subsequent analyses showed the mutation to be homozygous viable and fertile, with homozygotes expressing microphthalmia and closed eyes, and that the 132 mutation was allelic with three additional eye mutations. The allelism group was designated *Cat4* (Kratochvilova and Favor 1992) and the 132 mutation was previously assigned the mutant symbol *Apyc* or *Apcat1*. The 132 mutation was incorrectly (see results below) assigned linkage to chromosome (Chr) 8 (Favor *et al.* 1997).

Ophthalmological examinations were done as previously described (Favor 1983). Prior to mapping, a congenic C3H/HeJ 132 mutant line was established by >20 consecutive backcross generations of 132 heterozygotes to strain C3H/HeJ. Genomewide linkage analysis of the mutation relative to 42 Massachusetts Institute of Technology (MIT) microsatellite markers, which are distributed over the 19 autosomes, was carried out as previously described (Favor *et al.* 1997). Since, as will be shown below, the 132 mutation is a hypomorph mutant allele of *Pax6* with a high frequency of phenotypically misclassifying heterozygous carriers as wild type, only animals classified as mutants were used in the linkage analysis. After localization of the mutation to Chr 2 the backcross mice were genotyped for additional MIT microsatellite markers within the region. Segregation data were analyzed with Map Manager version 2.6.5 (Manly 1993) and the gene order was determined by minimizing the number of multiple crossovers. Animals were bred and maintained in our facilities according to the German law for the protection of animals. All inbred strains employed in this study (C3H/HeJ, C57BL/6El) were obtained from breeding colonies maintained by the Department of Animal Resources at Neuherberg.

Morphology and histology: Wild type, heterozygous 132/+ and homozygous 132/132 mutants were weighed, and both eyes were classified for the degree of eye opacity and eye weight at P35 as previously described (Favor *et al.* 2001), with the addition of two eye classes to accommodate the minor eye phenotype expressed by heterozygous 132/+ mice (minor iris irregularities with no lens opacity) and the extreme phenotype expressed by homozygous 132/132 mice (extreme microphthalmia with lens/corneal opacity and iris abnormality). Homozygous wild-type, heterozygous 132/+, and homozygous 132/132 embryos were produced from intercrosses of 132/+ heterozygotes. Compound heterozygotes were produced in crosses of homozygous 132/132 mutants with heterozygous carriers of various *Pax6* mutations. The recovered compound heterozygotes were fertility tested by outcrossing to homozygous wild-type and homozygous 132/132 mutant partners. Compound heterozygote embryos and animals at weaning were identified as expressing extreme microphthalmia. Embryos were collected and processed for histology, and histological sectioning, staining, and photography were all conducted as previously described (Favor *et al.* 2001, 2007).

Sequencing, DNA binding assay, and glucagon-promoter assay: RNA and genomic DNA were extracted from the heads and bodies, respectively, of homozygous wild-type and homozygous 132/132 mutant E15 embryos. Preparation and sequencing procedures were as previously described (Favor *et al.* 2001). Two primer pairs were used to generate overlapping amplification products across the *Pax6* cDNA. These amplification products were used as substrates to sequence the *Pax6* transcript. The sequencing results using cDNA as substrate were confirmed by sequencing the mutation site with genomic DNA as substrate in the initial embryos analyzed as well as from additional heterozygous and homozygous mutants. The primer pair used to amplify and to sequence the mutation site from genomic DNA was 5′ ACCCATTATCCAG ATGTGTTTGCC and 5′ GGAATGTGACTAGGAGTGTTGC TG. Numbering of the transcript and the translation products corresponds to EMSMUSG00000027168/ENUMUST000001 11087 (Ensembl, release 48).

The electrophoretic mobility-shift assay to ascertain homeodomain binding to the P3 DNA target was conducted as previously described (Favor *et al.* 2001). Briefly, subclones of the wild-type, $Pax6^{4Neu}$, and the 132 mutant *Pax6* cDNAs, coding for the entire homeodomain with six additional amino acids upstream and four amino acids downstream (*Pax6* amino acids 218–288), were inserted between the *Pst*I and the *Hin*dIII restriction sites of the pQE-41 vector (QIAGEN, Valencia, CA). The pQE expression constructs were transformed into *Escherichia coli* strain M15 [pREP4]. Expression of the homeodomains in exponentially growing bacterial cultures was induced with 0.1 mm isopropyl thiogalactoside for 2 hr at 30°. Bacterial pellets were lysed, crude extracts were electrophoresed in 10% SDS–PAGE, and proteins visualized by staining with Coomassie brilliant blue. Crude extracts from the transformed bacteria were incubated with 15 fmol of the target oligonucleotide, which was 3′ end labeled with digoxygenin-11-ddUTP as recommended by the supplier (Roche Diagnostics, Mannheim, Germany). The single-strand oligonucleotide target sequence (with the P3 homeodomain binding site underlined) was 5′TCGAGGGCATCAGGATG CTAATTGAATTAGCATCCGATCGGG3′, to which the *Pax6* homeodomain binds via cooperative dimerization (Wilson *et al.* 1993; Czerny and Busslinger 1995). The rabbit anti-Pax6-homeodomain antiserum used to control for the specificity of the homeodomain-DNA complex was serum 13 (Carrière *et al.* 1993).

To assess transcriptional activation by the *Pax6* wild-type, $Pax6^{4Neu}$, and 132 mutant gene products we carried out glucagon-promoter assays (Ritz-Laser *et al.* 1999; Planque *et al.* 2001). *Pax6* is expressed in the pancreas and is required for α-cell development and expression of glucagon (St-Onge

et al. 1997). Transcriptional activation of glucagon by *Pax6* is mediated by the interaction of *Pax6* with two AT-rich sequences, designated G1 and G3, of the glucagon gene (Ritz-Laser *et al.* 1999). The glucagon-promoter assay was carried out according to the previously described procedures (Ritz-Laser *et al.* 1999; Planque *et al.* 2001). The full-length wild-type, *Pax6^{4Neu}* mutant, and 132 mutant *Pax6* canonical transcripts (isoforms not containing the exon 5a) were amplified with the primer set 5′ AGCTCCAGCATGCAGAACAGTCAC and 5′ ACTGCTGTGTCCACATAGTCATTGGC using the Titan RT–PCR system (Roche Diagnostics, Mannheim, Germany). The amplification products were isolated by electrophoretic separation in 1% agarose gels and extracted with the MiniElute kit (QIAGEN). The blunt-end PCR products were modified to sticky-end 3′ A overhangs with the QIAGEN PCR Cloning^{plus} kit (QIAGEN) and ligated into the QIAGEN pDrive Cloning Vector orientated to the T7 promoter (QIAGEN). Transformed *E. coli* strain M15[pREP4] colonies were isolated, cultured, and plasmid DNA extracted for sequencing to identify clones containing the full-length transcript sequences correctly orientated to the T7 promoter. The *Kpn*I–*Hin*dIII restriction fragment of each clone containing the entire *Pax6* coding sequence was inserted into the pVNC vector. *Pax6* was therefore expressed under the control of the CMV promoter. BHK-21 cells were co-transfected with DNA from a CAT reporter gene construct driven by the −138 glucagon promoter bearing the G1 *Pax6*-binding element, a *Pax6* expression vector containing the full-length open reading frame of the mouse wild-type, *Pax6^{4Neu}* mutant, or the *Pax6$^{132\text{-}14Neu}$* mutant cDNA sequence, and the pcDNA3-LacZ vector (for normalization of the CAT assay). The −138 glucagon promoter is a 196-bp sequence from the proximal region of the glucagon gene. The G1 sequence containing two 7-bp AT-rich sequences (underlined) within the −138 promoter was 5′ CCCCATTATTTACAGATGAGAAATTTATATTGT (Ritz-Laser *et al.* 1999). The CAT assays were performed as previously described (Plaza *et al.* 1999).

RESULTS

Breeding, eye morphology, and mapping: In an attempt to increase the accuracy of our initial linkage studies (Favor *et al.* 1997) we noted that the mutation was not linked to Chr 8. We undertook another genomewide mapping study and localized the 132 mutation to Chr 2 with the following locus order (frequencies of crossovers between adjacent loci are given in parentheses): *D2Mit249*-(1/71)-132-(1/71)-*D2Mit102*-(2/71)-*D2Mit258*-(13/71)-*Agouti*. On the basis of the chromosomal region and the eye phenotype we considered *Pax6* to be a candidate gene for mutation analysis. Sequencing analyses confirmed the 132 mutation to be a nucleotide substitution (c.T1099A) within the coding region of the *Pax6* gene. The base-pair substitution results in an amino acid substitution (Phe272Ile) within the third helix of the homeodomain. We have assigned the mutation the allele symbol *Pax6$^{132\text{-}14Neu}$*, which has been approved by the Mouse Genetic Nomenclature Committee (accession no. MGI: 1856585). Heterozygous *Pax6$^{132\text{-}14Neu}$* mutant embryos expressed microphthalmia, anterior pyramidal opacity, adhesion of the lens to the cornea, and a reduced anterior chamber (Figure 3D). Homozygous *Pax6$^{132\text{-}14Neu}$* mutant embryos expressed extreme microphthalmia with more extreme lens and corneal defects than observed in heterozygotes (Figure 3H).

TABLE 1

Characterization of eye phenotypes in P35 *Pax6$^{132\text{-}14Neu}$* mutant mice

	Eye class (%)[b]					
Genotype[a]	0	Minor iris abnormalities	25	50	75	100 Extreme microphthalmia
+/+	118					
+/−	38	190	28	4		
−/−						32

[a] +/+ were wild-type strain C3H mice; +/− mice were produced in the cross −/− × +/+; −/− mice were from the cross −/− × −/−.

[b] Classes 0, 25, 50, 75, and 100% denote lens/corneal opacities affecting 0, 25, 50, 75 or 100% of the eye, respectively.

We confirmed that the *Pax6$^{132\text{-}14Neu}$* mutation is homozygous viable and that heterozygous and homozygous mutants are fully fertile with no significant differences ($F_{3,145} = 1.33$, $P = 0.26$) in average litter size among the various crosses (+/− × +/+, 5.77 ± 0.32, $n = 57$; +/− × +/−, 4.76 ± 0.52, $n = 25$; −/− × +/+, 5.80 ± 0.56, $n = 20$; −/− × −/−, 5.83 ± 0.30, $n = 47$). The frequency of presumed heterozygous carriers was less than expected on the basis of a phenotypic classification of offspring (data not shown). We carefully characterized the eye phenotypes in P35 animals of known genotype. In heterozygous *Pax6$^{132\text{-}14Neu}$* mutants there was a high frequency of eyes with no observable defects or with only minor iris irregularities, which fall outside the range of eye phenotypes previously associated (Favor *et al.* 2001) with heterozygous *Pax6* mutants (Table 1), and eye size was slightly reduced (+/+, 18.90 mg ± 0.07, $n = 116$; +/−, 16.68 mg ± 0.05, $n = 259$). This observation explains the distortion in the ratio of presumed wild-type and heterozygous mutant carriers when classified phenotypically according to our previous classification criteria for *Pax6* mutants (Favor *et al.* 2001). All homozygous *Pax6$^{132\text{-}14Neu}$* mutants expressed extreme microphthalmia with lens/corneal opacity and iris abnormality (Table 1) and eye weight was extremely reduced (−/−, 2.88 mg ± 0.12, $n = 32$). Body weight (+/+, 19.49 g ± 0.24, $n = 58$; +/−, 17.94 g ± 0.18, $n = 128$; −/−, 17.96 g ± 0.29, $n = 16$) of heterozygous and homozygous *Pax6$^{132\text{-}14Neu}$* mutants was less than the body weight of homozygous wild types (+/+ *vs.* +/−, $t = 4.94$, $P_{\text{two-tailed}} = 1.73 \times 10^{-6}$, d.f. = 184; +/+ *vs.* −/−, $t = 3.20$, $P_{\text{two-tailed}} = 0.002$, d.f. = 72). Since mutant *Pax6$^{132\text{-}14Neu}$* mice were associated with a significant reduction in body size, eye weights were normalized for body weight (Table 2). As compared to wild type, the normalized eye weight of heterozygous

TABLE 2

Normalized eye weight in P35 *Pax6*$^{132\text{-}14Neu}$ mutant mice

	Normalized eye weight[b]				
Genotype[a]	*N*	Mean	SEM	Minimum	Maximum
+/+	116	9.76	0.07	8.4	11.8
+/−	255	9.44	0.09	5.9	22.1
−/−	32	1.61	0.07	1.1	2.7

[a] Genotype origins as in Table 1.
[b] Normalized eye weight = [(eye weight (mg)/body weight (g)) × 10].

Pax6$^{132\text{-}14Neu}$ mutants was moderately but significantly reduced ($t = 2.30$, $P_{\text{two-tailed}} = 0.02$, d.f. = 369). The normalized eye weight of homozygous *Pax6*$^{132\text{-}14Neu}$ mutants was extremely reduced ($t = 58.37$, $P_{\text{two-tailed}} = 4.27 \times 10^{-103}$, d.f. = 146).

DNA-binding and glucagon-promoter activation associated with the *Pax6*$^{132\text{-}14Neu}$ gene product: Given the functional significance of the third helix of the homeodomain (Hanes and Brent 1989; Treisman *et al.* 1989; Wilson *et al.* 1993; Gehring *et al.* 1994; Qian *et al.* 1994; Bruun *et al.* 2005), we characterized the binding activity of the *Pax6*$^{132\text{-}14Neu}$ mutant homeodomain to the P3 target sequence and the glucagon-promoter activation of the *Pax6*$^{132\text{-}14Neu}$ gene product. Results indicated loss of binding activity of the *Pax6*$^{132\text{-}14Neu}$ mutant homeodomain to the P3 DNA binding target (Figure 1). The glucagon-promoter activation by the mutant *Pax6*$^{132\text{-}14Neu}$ was slightly higher than wild-type *Pax6* (transformations with 100 ng DNA: wild type, 7.19 ± 0.19, $n = 2$; *Pax6*$^{132\text{-}14Neu}$, 10.87 ± 0.31, $n = 2$, $t = 14.31$, $P_{\text{two-tailed}} < 0.05$; transformations with 300 ng DNA: wild type, 8.49 ± 0.64, $n = 2$; *Pax6*$^{132\text{-}14Neu}$, 11.74 ± 0.23, $n = 2$, $t = 6.75$, $P_{\text{two-tailed}} < 0.05$) (Figure 2). In these assays we included a previously described *Pax6* hypomorph mutation, *Pax6*^{4Neu}, also due to an amino acid substitution within the third helix of the homeodomain (Ser273-Pro). We observed that the binding activity of the *Pax6*^{4Neu} mutant homeodomain to the P3 target sequence was ablated (Figure 1) and there was greatly reduced glucagon-promoter activation by the mutant *Pax6*^{4Neu} (transformations with 100 ng DNA: wild type, 7.19 ± 0.19, $n = 2$; *Pax6*^{4Neu}, 2.15 ± 0.12, $n = 2$, $t = 31.75$, $P_{\text{two-tailed}} < 0.05$; transformations with 300 ng DNA: wild type, 8.49 ± 0.64, $n = 2$; *Pax6*^{4Neu}, 3.29 ± 0.44, $n = 2$, $t = 9.47$, $P_{\text{two-tailed}} < 0.05$) (Figure 2). Cotransfection of cells with mutant *Pax6*^{4Neu} and wild-type *Pax6* indicated that the mutant *Pax6*^{4Neu} did not interfere with the normal promoter activation of the wild-type *Pax6*. Taken together, these results indicate that the *Pax6*$^{132\text{-}14Neu}$ and *Pax6*^{4Neu} missense mutations in the third helix of the homeodomain both affect the binding activities of the mutant homeodomains. However, whereas the glucagon-promoter activity of the *Pax6*$^{132\text{-}14Neu}$ gene product was increased, the activity of the *Pax6*^{4Neu} gene product was greatly reduced. Since the reporter gene employed for this assay was driven by the G1 *Pax6* paired and homeodomain binding site (Planque *et al.* 2001) our results suggest that dysfunction due to the *Pax6*$^{132\text{-}14Neu}$ missense mutation is confined to the homeodomain and allowed transcriptional activation by the intact paired domain, while the *Pax6*^{4Neu} homeodomain missense mutation also affects the binding activity of the gene product to paired domain targets.

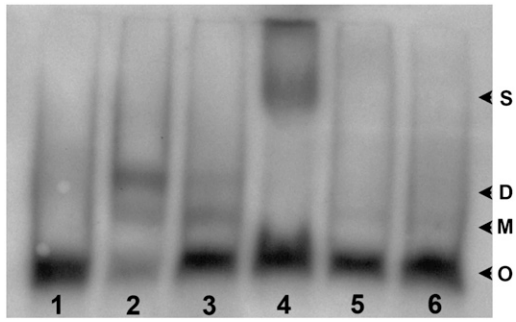

Figure 1.—Binding activity of the wild-type, *Pax6*^{4Neu}, and *Pax6*$^{132\text{-}14Neu}$ *Pax6*-homeodomains to the P3 DNA target sequence. Whole cell extracts from the transformed *E. coli* strain M15[pREP4] were incubated with 15 fmol of the digoxygenin-labeled P3 target oligonucleotide. Binding specificity was demonstrated by competition of the labeled P3 target oligonucleotide with an excess of unlabeled P3 target oligonucleotide and a supershift assay with the *Pax6* homeodomain-specific antibody. (Lane 1) P3 oligonucleotide alone; (lane 2) P3 oligonucleotide with 50 ng wild-type *Pax6* homeodomain; (lane 3) P3 oligonucleotide with 50 ng wild-type *Pax6* homeodomain and 3.3 pmol unmarked P3 oligonucleotide; (lane 4) P3 oligonucleotide with 50 ng wild-type *Pax6* homeodomain and 2 μl of the *Pax6* homeodomain-specific antiserum; (lane 5) P3 oligonucleotide with 50 ng mutant *Pax6*^{4Neu} homeodomain; (lane 6) P3 oligonucleotide with 50 ng mutant *Pax6*$^{132\text{-}14Neu}$ homeodomain. The positions of the free oligonucleotide (O), the monomeric (M), and dimeric (D) DNA-protein complexes, and the shifted antibody DNA-protein complex (S) are marked.

Compound heterozygotes: We next attempted to produce compound *Pax6* heterozygotes with *Pax6*$^{132\text{-}14Neu}$ and two previously described *Pax6* hypomorph alleles (*Pax6*^{4Neu} and *Pax6*^{7Neu}), which are more severely affected than carriers of the *Pax6*$^{132\text{-}14Neu}$ mutation (Favor *et al.* 2001) or with the previously described null alleles *Pax6*$^{Sey\text{-}Neu}$, *Pax6*^{2Neu}, and *Pax6*^{3Neu} (Favor *et al.* 2001; Hill *et al.* 1991) (Table 3). All compound heterozygote combinations expressed extreme microphthalmia and were viable, and the compound heterozygotes *Pax6*^{2Neu}/*Pax6*$^{132\text{-}14Neu}$, *Pax6*^{4Neu}/*Pax6*$^{132\text{-}14Neu}$, *Pax6*^{7Neu}/*Pax6*$^{132\text{-}14Neu}$, and *Pax6*$^{Sey\text{-}Neu}$/*Pax6*$^{132\text{-}14Neu}$ were fertile. The compound heterozygote *Pax6*^{3Neu}/*Pax6*$^{132\text{-}14Neu}$ was not fertility tested.

In previous characterizations of our extensive *Pax6* allelic series we have concluded that most alleles (*Pax6*$^{Sey\text{-}Neu}$, *Pax6*^{2Neu}, *Pax6*^{3Neu}, *Pax6*^{5Neu}, *Pax6*^{6Neu}, *Pax6*^{8Neu}, *Pax6*^{9Neu}, *Pax6*^{10Neu}, and *Pax6*^{Coop}) result in premature truncation of the *Pax6* translation product (Hill *et al.* 1991; Lyon *et al.* 2000; Favor *et al.* 2001). The hypomorph alleles

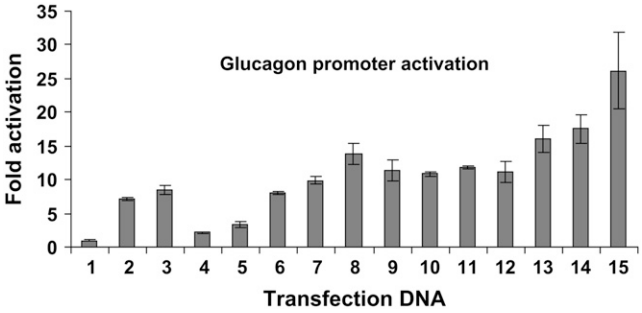

FIGURE 2.—Glucagon-promoter activation by wild-type, $Pax6^{4Neu}$ and $Pax6^{132\text{-}14Neu}$ gene products. A CAT assay was employed to measure the glucagon-promoter activity of the wild-type or mutant Pax6 in BHK-21 cotransfected cells. CAT activities were normalized to β-galactosidase activity obtained from cotransfection with the LacZ expression vector. Fold activation represents the observed normalized CAT activities relative to the normalized CAT activity in cells cotransfected with the empty expression plasmid DNA. (Lane 1) cells transfected with 100 ng empty plasmid DNA; (lanes 2 and 3) cells transfected with 100 ng (lane 2) or 300 ng (lane 3) wild-type *Pax6* plasmid DNA constructs; (lanes 4 and 5) cells transfected with 100 ng (lane 4) or 300 ng (lane 5) mutant $Pax6^{4Neu}$ plasmid DNA constructs; (lanes 6–9) cells cotransfected with plasmid DNA from wild-type *Pax6* and mutant $Pax6^{4Neu}$ constructs: (lane 6) 100 ng DNA from wild-type *Pax6* and 100 ng from mutant $Pax6^{4Neu}$; (lane 7) 100 ng DNA from wild-type *Pax6* and 300 ng from mutant $Pax6^{4Neu}$; (lane 8) 300 ng DNA from wild-type *Pax6* and 100 ng from mutant $Pax6^{4Neu}$; (lane 9) 300 ng DNA from wild-type *Pax6* and 300 ng from mutant $Pax6^{4Neu}$; (lanes 10 and 11) cells transfected with 100 ng (lane 10) or 300 ng (lane 11) DNA from mutant $Pax6^{132\text{-}14Neu}$ plasmid constructs; (lanes 12–15) cells cotransfected with plasmid DNA from wild-type *Pax6* and mutant $Pax6^{132\text{-}14Neu}$ constructs: (lane 12) 100 ng DNA from wild-type *Pax6* and 100 ng from mutant $Pax6^{132\text{-}14Neu}$; (lane 13) 100 ng DNA from wild-type *Pax6* and 300 ng from mutant $Pax6^{132\text{-}14Neu}$; (lane 14) 300 ng DNA from wild-type *Pax6* and 100 ng from mutant $Pax6^{132\text{-}14Neu}$; (lane 15) 300 ng DNA from wild-type *Pax6* and 300 ng from mutant $Pax6^{132\text{-}14Neu}$. Columns represent mean ± SD fold activation from two determinations.

$Pax6^{4Neu}$ and $Pax6^{7Neu}$ express delayed perinatal lethality when compared with homozygous *Pax6* null mutations (FAVOR *et al.* 2001), and thus they must have less *Pax6* activity than the $Pax6^{132\text{-}14Neu}$ mutation, which is homozygous viable and fertile. The phenotype expressed by homozygous mutant $Pax6^{132\text{-}14Neu}$ mice was more severe than that of heterozygous *Pax6* null mutants, and therefore $Pax6^{132\text{-}14Neu}$ homozygous mutants must express <50% *Pax6* activity. Since the compound heterozygotes of $Pax6^{132\text{-}14Neu}$ carried over *Pax6* null alleles are viable and fertile, a single copy of the $Pax6^{132\text{-}14Neu}$ mutation carried over a null allele must have more activity than two copies of $Pax6^{4Neu}$ or $Pax6^{7Neu}$ carried by the respective homozygotes. On the basis of these results we could predict the order of *Pax6* activity in wild-type and mutant *Pax6* genotypes as follows: *Pax6* $+/+ = 100\% > Pax6^{132\text{-}14Neu}/+ > Pax6^{3Neu}/+ = 50\% > Pax6^{132\text{-}14Neu}/Pax6^{132\text{-}14Neu} > Pax6^{4Neu}/Pax6^{132\text{-}14Neu} \approx Pax6^{7Neu}/Pax6^{132\text{-}14Neu} > Pax6^{3Neu}/Pax6^{132\text{-}14Neu} > Pax6^{7Neu}/Pax6^{7Neu} > Pax6^{3Neu}/Pax6^{3Neu} = 0\%$. We constructed these genotypes and assessed the degree of eye development in E15 embryos when the expected *Pax6* activity in the embryos ranged from 100% normal to 0% (Figure 3). Results indicated that the degree of eye development is progressively affected as the expected *Pax6* activity is reduced. Considering the degree of eye development, the various genotypes assessed can be grouped into three distinct classes. In the first class, embryos have a higher predicted Pax6 activity [*Pax6* +/+ (A and B), $Pax6^{132\text{-}14Neu}/+$ (C and D), $Pax6^{3Neu}/+$ (E and F), and $Pax6^{132\text{-}14Neu}/Pax6^{132\text{-}14Neu}$ (G and H)] and the basic eye plan developed with a definite cornea, lens, and retina. However, as the predicted level of *Pax6* activity was reduced there was a progressive reduction in eye size and the degree of anterior segment abnormalities increased (thickened cornea, failure of the lens to detach from the cornea, degree of development of the anterior chamber between the cornea and lens). The second class [$Pax6^{4Neu}/Pax6^{132\text{-}14Neu}$ (I and J) and $Pax6^{7Neu}/Pax6^{132\text{-}14Neu}$ (K and L)] consists of embryos with less predicted *Pax6* activity than that in the first class. A rudimentary eye developed consisting of a retina and a distinct optic pit. However, there was no apparent invagination of the surface ectoderm into the optic cup nor was there development of lenticular tissue. The third class consists of embryos with the least predicted *Pax6* activity [$Pax6^{3Neu}/Pax6^{132\text{-}14Neu}$ (M and N), $Pax6^{7Neu}/Pax6^{7Neu}$ (O and P), and $Pax6^{3Neu}/Pax6^{3Neu}$ (Q and R)]. In all three genotypes within this class the tissue observed had no apparent resemblance to a rudimentary eye. The progression of eye development in the genotype within this class with the higher predicted activity [$Pax6^{3Neu}/Pax6^{132\text{-}14Neu}$ (M and N)] was more extensive with more tissue derived from the optic vesicle in the vicinity of the surface ectoderm and an apparent rudimentary optic pit. By comparison, there was minimal progression of eye development in the genotype with zero *Pax6* activity [$Pax6^{3Neu}/Pax6^{3Neu}$ (Q and R)]. The tissue derived from the optic vesicle (arrowheads) was observed to be distant from the surface ectoderm and there was no evidence of the formation of a rudimentary optic pit. The $Pax6^{7Neu}/Pax6^{7Neu}$ genotype (O and P) with predicted *Pax6* activity between the other two genotypes in this class expressed an intermediate progression in eye development.

DISCUSSION

In this study we have characterized a *Pax6* missense hypomorph mutant allele and, utilizing our extensive *Pax6* mutant allelic series, constructed genotypes such that the predicted *Pax6* activity varied between 100 and 0%. We show that the extent of eye development was directly related to the levels of *Pax6* activity. The genotypes may be grouped into three distinct classes that define apparent thresholds in the relationship

TABLE 3

Recovery and fertility testing of *Pax6* compound heterozygotes

Cross	Phenotype class (%)[a]		
	0	Minor iris anomaly, 25, 50, 75, or 100	Extreme microphthalmia
$Pax6^{4Neu-/+} \times Pax6^{132\text{-}14Neu-/-}$	2	16	11
$Pax6^{4Neu}/Pax6^{132\text{-}14Neu} \times +/+$	3	24	—
$Pax6^{4Neu}/Pax6^{132\text{-}14Neu} \times Pax6^{132\text{-}14Neu-/-}$	—	—	36
$Pax6^{7Neu-/+} \times Pax6^{132\text{-}14Neu-/-}$	1	9	9
$Pax6^{7Neu}/Pax6^{132\text{-}14Neu} \times +/+$	—	29	—
$Pax6^{7Neu}/Pax6^{132\text{-}14Neu} \times Pax6^{132\text{-}14Neu-/-}$	—	—	10
$Pax6^{Sey\text{-}Neu-/+} \times Pax6^{132\text{-}14Neu-/-}$	2	14	5
$Pax6^{Sey\text{-}Neu}/Pax6^{132\text{-}14Neu} \times +/+$	1	11	—
$Pax6^{Sey\text{-}Neu}/Pax6^{132\text{-}14Neu} \times Pax6^{132\text{-}14Neu-/-}$	—	—	20
$Pax6^{2Neu-/+} \times Pax6^{132\text{-}14Neu-/-}$	—	16	8
$Pax6^{2Neu}/Pax6^{132\text{-}14Neu} \times +/+$	—	26	—
$Pax6^{2Neu}/Pax6^{132\text{-}14Neu} \times Pax6^{132\text{-}14Neu-/-}$	—	—	9
$Pax6^{3Neu-/+} \times Pax6^{132\text{-}14Neu-/-}$	—	9	7

[a] Phenotype classes are as in Table 1.

between *Pax6* activity and an abrupt shift in the extent of eye development. The first threshold at which *Pax6* activity was <50% demarks a shift from development of a complete eye in genotypes above the threshold to a group of genotypes that develops only a rudimentary eye consisting of a retina and no lenticular tissue. The second threshold at a very low level of *Pax6* activity is associated with a shift from development of a rudimentary eye in genotypes with higher levels of *Pax6* to a group of genotypes in which eye development terminated very early and the tissues had no resemblances to a rudimentary eye.

Hypomorph *Pax6*$^{132\text{-}14Neu}$ allele: We show that heterozygous carriers of the *Pax6*$^{132\text{-}14Neu}$ mutation express minor eye abnormalities and homozygous mutants are viable and fertile. These results extend the mouse *Pax6* allelic series to include a hypomorph mutant allele with a level of *Pax6* residual activity sufficient for homozygous and hemizygous mutants to be viable and fertile. We have previously described two hypomorph alleles, *Pax6*^{4Neu} and *Pax6*^{7Neu}, in which homozygous embryos express more optic tissues than that seen in homozygous *Pax6* null mutants and there was delayed time of perinatal death (Favor *et al.* 2001). The site of the *Pax6*$^{132\text{-}14Neu}$ missense mutation, Phe272Ile, is in the third helix of the homeodomain and is highly conserved across all paired-like homeodomain sequences. The aromatic sidechain is buried within the protein tertiary

Figure 3.—The extent of eye development in mutant *Pax6* genotype constructs with varying levels of predicted *Pax6* activity. From the *Pax6* allelic series we have utilized *Pax6* wild type, the *Pax6*^{3Neu} null (a frameshift mutation that ablates the linker, homeodomain, and transactivation domain (Favor *et al.* 2001), the *Pax6*^{4Neu} hypomorph (a homeodomain missense mutation that ablates homeodomain binding and reduces translation activation at paired domain target sites (Favor *et al.* 2001; this study), the *Pax6*^{7Neu} hypomorph (a Kozak sequence mutation that greatly reduces translation levels of Pax6 (Favor *et al.* 2001) and the *Pax6*$^{132\text{-}14Neu}$ hypomorph (this study) alleles. The genotypes are arranged from top to bottom in a descending order of predicted *Pax6* activity. The genotypes in A and B (wild type) up to and including M and N (*Pax6*$^{3Neu}/Pax6^{132\text{-}14Neu}$) are viable and fertile. The genotypes in O and P (*Pax6*$^{7Neu}/Pax6^{7Neu}$) and Q and R (*Pax6*$^{3Neu}/Pax6^{3Neu}$) are lethal. Regions at which there was an abrupt shift in the extent of eye development are indicated by horizontal lines and identify three groups: class 1, highest levels of *Pax6* activity and eye development was complete; class 2, intermediate levels of *Pax6* activity and a rudimentary eye developed; class 3, lowest levels of *Pax6* activity and eye development terminated very early. Head overview (A, C, E, G, I, K, M, O, and Q) and eye (B, D, F, H, J, L, N, P, and R) histology of E15 wild-type and *Pax6* mutant constructs. Eye development is normal in homozygous wild-type (A and B) embryos with 100% *Pax6* activity, showing a well-developed cornea (co), lens (le), retina (ret), and a distinct anterior chamber between the cornea and the anterior surface of the lens. In heterozygous *Pax6*$^{132\text{-}14Neu}$ embryos (C and D) with *Pax6* activity >50% but <100% eye size is slightly reduced and the separation of the anterior surface of the lens from the cornea is incomplete resulting in a reduced anterior chamber. Heterozygotes of the *Pax6*^{3Neu} null mutation (E and F) with 50% *Pax6* activity show a further reduction in eye size as compared to heterozygous *Pax6*$^{132\text{-}14Neu}$ mutants, the lens remains attached to the cornea, there is no anterior chamber, and a plug of persistent epithelial cells remains in the cornea (arrow). Homozygous *Pax6*$^{132\text{-}14Neu}$ mutants (G and H) have <50% *Pax6* activity. All major eye tissues (cornea, lens, and retina) develop. However eye size is reduced and there is a large plug of persistent epithelial cells that remains attached between the cornea and the lens (arrow). Compound heterozygotes between *Pax6*$^{132\text{-}14Neu}$ and the hypomorph *Pax6*^{4Neu} (I and J) or *Pax6*^{7Neu} (K and L) mutant alleles have *Pax6* activity less than that in homozygous *Pax6*$^{132\text{-}14Neu}$ mutants. Eye development is incomplete. The optic

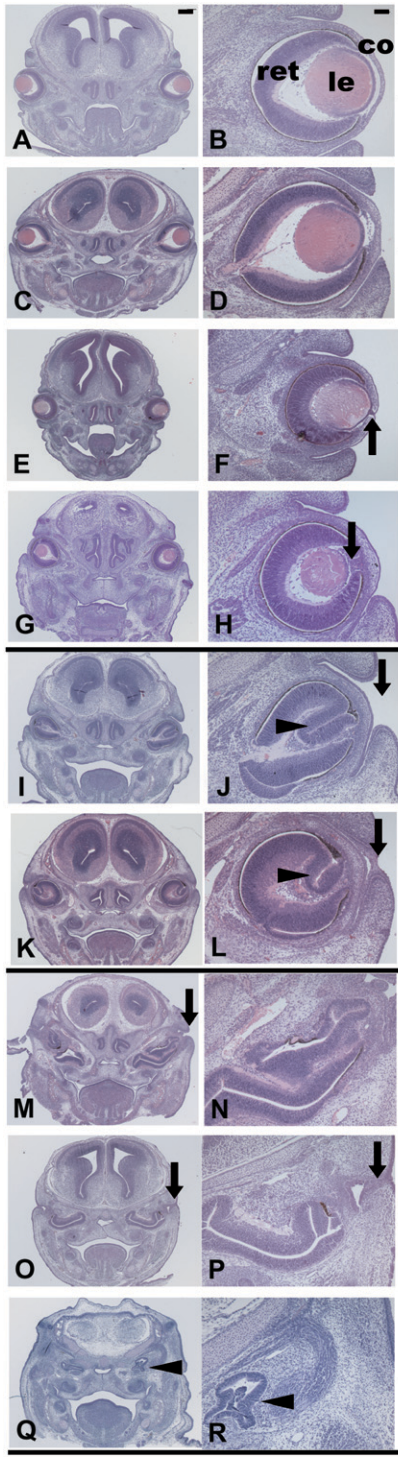

Genotype	Pax6 activity	Class
Pax6$^{+/+}$	100%	1 = eye plan complete
Pax6$^{14Neu/+}$	<100%, >50%	1
Pax6$^{3Neu/+}$	50%	1
Pax6$^{14Neu/14Neu}$	<50%	1
Pax6$^{4Neu/14Neu}$	<50%	2 = retina present, lens vesicle did not develop
Pax6$^{7Neu/14Neu}$	<50%	2
Pax6$^{3Neu/14Neu}$	<50%, > 0%	3 = very early termination of eye development
Pax6$^{7Neu/7Neu}$	>0%	3
Pax6$^{3Neu/3Neu}$	0%	3

vesicle makes contact with the surface ectoderm and a retina is formed with characteristic displacements in the dorsal tip region (arrowheads). A distinct optic pit is present (arrows). However the lens placode does not invaginate and there are no lenticular tissues. Compound heterozygote *Pax6*^{3Neu}/*Pax6*$^{132\text{-}14Neu}$ embryos (M and N) have less *Pax6* activity than that in the *Pax6*^{4Neu}/*Pax6*$^{132\text{-}14Neu}$ or *Pax6*^{7Neu}/*Pax6*$^{132\text{-}14Neu}$ compound heterozygotes and eye development terminates at an earlier stage. The optic vesicle appears to have made contact with the surface ectoderm but contact has not been maintained, there is no apparent invagination of the optic vesicle to initiate formation of an optic cup, there is only a rudimentary response of the surface ectoderm to form an optic pit (arrow), and apparently no lenticular tissue develops from the presumptive lens placode. *Pax6* activity in *Pax6*^{7Neu} homozygous mutants (O and P) is less than that in *Pax*^{3Neu}/*Pax6*$^{132\text{-}14Neu}$ and eye development terminates at a very early stage. There is no invagination of the optic vesicle, a very rudimentary response of the surface ectoderm (arrows), and no apparent invagination of the presumptive lens placode to form lenticular tissue. Homozygous *Pax6*^{3Neu} mutants (Q and R) have 0% *Pax6* activity and although optic vesicle development is initiated it terminates extremely early and the resultant tissue (arrowheads) was displaced and found extremely distant from the surface ectoderm. There was no observed initial invagination of the surface ectoderm. Bar in A represents 400 μm and bar in B represents 100 μm.

structure in close proximity to a second Phe site from helix 1 of the homeodomain and may participate in stabilizing the homeodomain tertiary structure. The third helix of the homeodomain makes direct contact to the DNA and our observation that the binding activity of the mutant *Pax6*$^{132\text{-}14Neu}$ homeodomain to the P3 target DNA sequence is lost is compatible with the conclusion that the Phe272Ile missense mutation alters the tertiary structure of the homeodomain and prevents proper binding to the DNA target.

The glucagon-promoter activity assays of the full-length *Pax6* wild-type and mutant gene products employed the CAT expression vector driven by the −138 glucagon promoter. This promoter contains the G1 sequence, which is a target site for binding of the *Pax6* paired and homeodomains and the paired domain alone is sufficient for activation when the homeodomain is deleted from the *Pax6* gene product (Ritz-Laser *et al.* 1999; Planque *et al.* 2001). We observed that the glucagon-promoter activity of the mutant *Pax6*$^{132\text{-}14Neu}$ gene product was slightly increased. Thus, the mutated Phe272Ile site in the homeodomain may result in an increase of the glucagon-promoter activation via the paired domain in the mutant *Pax6* product. In contrast, the Ser273Pro *Pax6*^{4Neu} missense mutation, also within the third α-helix of the homeodomain, has reduced glucagon-promoter activation in the CAT reporter gene construct driven by the −138 glucagon promoter. This indicates that this mutation, which is predicted to interrupt the third α-helix structure (Favor *et al.* 2001), also affects the glucagon-promoter activation via the paired domain. It likely does not affect Pax6 dimerization since it did not affect the wild-type *Pax6* glucagon-promoter activation in the *Pax6* wild type + *Pax6*^{4Neu} cotransfection assays. Rather, we interpret these results to indicate that, within the *Pax6*^{4Neu} mutant gene product, the mutant *Pax6* homeodomain interferes with the paired domain DNA binding activity to the paired domain target sites.

The third hypomorph mutant allele utilized in this study, *Pax6*^{7Neu}, has been shown to be a c.A-3T base-pair substitution outside the *Pax6* ORF in the Kozak sequence and results in greatly reduced translation product (Favor *et al.* 2001).

Correlation of *Pax6* activity and the extent of eye development: Previous studies have shown that normal eye development requires a narrow range of *Pax6* activity. Heterozygous null mutations (Hill *et al.* 1991) as well as transgenic mice that overexpress *Pax6* (Schedl *et al.* 1996) were associated with abnormal eye development. The identification of the *Pax6*$^{132\text{-}14Neu}$ hypomorph mutation, which is homozygous viable and has a higher level of *Pax6* activity than the *Pax6*^{4Neu} or *Pax6*^{7Neu} hypomorph alleles, has extended the range of the mouse *Pax6* allelic series. With the availability of an extended *Pax6* allelic series we were able to construct wild-type and mutant *Pax6* genotypes, which provides information regarding the extent of eye development and animal viability for four new levels of predicted *Pax6* activity: one genotype (*Pax6*$^{132\text{-}4Neu}$/+) with *Pax6* activity between 100 and 50% and three genotypes within the critical region between 50 and 0% *Pax6* activity (*Pax6*$^{132\text{-}4Neu}$/*Pax6*$^{132\text{-}4Neu}$, *Pax6*$^{132\text{-}14Neu}$/*Pax6*^{4Neu} ∼ *Pax6*$^{132\text{-}14Neu}$/*Pax6*^{7Neu}, *Pax6*$^{132\text{-}14Neu}$/*Pax6*^{3Neu}). We observed that as the level of predicted *Pax6* activity was reduced there was a progressive reduction in the extent of eye development. In the early stages of eye development two regions in the head critical for eye development show *Pax6* expression: the early optic vesicle and the surface ectoderm. Studies in the chick have shown that the regional localization of the *Pax6*-positive cells in the surface ectoderm is independent of a neighboring *Pax6*-positive optic vesicle (Li *et al.* 1994). The early optic vesicle is an evagination of the prospective forebrain and makes contact with the *Pax6*-positive region of the surface ectoderm. Upon contact of the optic vesicle with the surface ectoderm, the optic vesicle invaginates to form the optic cup, consisting of the outer layer (presumptive pigmented retinal layer) and the inner layer (presumptive neural retina layer). The lens placode, which is the *Pax6*-positive surface ectoderm at the region of contact between the optic vesicle and the surface ectoderm, invaginates into the optic cup to form the lens vesicle. In the class of genotypes with the highest level of predicted *Pax6* activity the basic eye plan developed, consisting of a cornea, lens, and retina. Thus, within this group of genotypes the levels of *Pax6* activity were sufficient for the optic vesicle to make proper contact with the *Pax6*-positive surface ectoderm and the lens placode was competent to invaginate and form a lens.

The second group of mutant genotypes had an intermediate level of predicted Pax6 activity. The optic vesicle evaginated toward and maintained contact with the surface ectoderm. A retina developed but the presumptive lens placode of the surface ectoderm did not invaginate and form the lens vesicle. Conditional inactivation of *Pax6* in a stage- and cell-specific manner has shown that at later stages the developmental competency of eye tissues depends upon the endogenous *Pax6* activity of the cells from which the tissues are derived. Inactivation of a single copy of *Pax6* in the distal optic cup allows proper development of the lens and cornea but developmental abnormalities of the iris were observed. Similarly, inactivation of a single copy of *Pax6* in the lens placode resulted in abnormal lens and cornea development. Retina development was normal and there were only mild noncell-autonomous iris abnormalities (Davis-Silberman *et al.* 2005). Microsurgical removal of the *Pax6*-positive neural plate and thus ablation of optic vesicle development in the chick resulted in *Pax6*-positive surface ectoderm cells but lens development was blocked (Li *et al.* 1994). Inactivation of *Pax6* in the early optic vesicle of the chick resulted in death of the optic vesicle cells and blocked lens

development from the *Pax6*-positive surface epithelium (Canto-Soler and Adler 2006). Thus, the maintenance of *Pax6* expression in the surface ectoderm is not dependent upon optic vesicle contact, but when optic vesicle contact to the surface ectoderm is prevented lens development is blocked. Complete inactivation of *Pax6* in the lens placode blocked lens development. Multiple, fully differentiated retinae were observed within the optic cup indicating that the presence of a lens was not required for the development of the retina (Ashery-Padan *et al.* 2000). Our observations for the second class of genotypes with intermediate levels of *Pax6* activity are compatible with the hypothesis that the levels of *Pax6* activity in the optic vesicle and the surface ectoderm were sufficient for retina development but were insufficient for development of the lens vesicle.

In the class of mutant genotypes with the lowest levels of predicted *Pax6* activity, the levels of *Pax6* activity were insufficient for proper eye development beyond a very early stage. Although there was an initiation of optic vesicle development, it terminated very prematurely and the resultant tissue had no resemblance to a rudimentary eye.

Taken together, these results indicate that the level of *Pax6* activity is less critical for the progression of optic vesicle evagination and retina development than it is for the invagination of the lens placode to develop into the lens vesicle. Characterization of the $Pax6^{Sey}$ null mutation (Hogan *et al.* 1986) demonstrated that in homozygous mutant embryos evagination of the optic vesicle was initiated but contact with the surface ectoderm was lost at a very early stage. Studies utilizing $Pax6^{-/-} \leftrightarrow Pax6^{+/+}$ chimera have shown that upon contact of the optic vesicle to the surface ectoderm *Pax6* activity deduced from the fraction of $Pax6^{+/+}$ and $Pax6^{-/-}$ cells in both the optic vesicle and the surface ectoderm is critical for the maintenance of this contact and for the induction of a lens placode (Collinson *et al.* 2000). Thus, lens development requires maintenance of the contact of the optic vesicle with the surface ectoderm and proper lens development is dependent upon *Pax6* activity in both structures.

Although we have assigned abstract relative *Pax6* activity levels to the *Pax6* mutant alleles on the basis of viability of mutant genotypes, the actual situation is more complex due to the spectrum of genes targeted for activation by the different isoforms of the mutant alleles. Despite our simplistic notion of predicted *Pax6* activity, it was very convincing to observe that the extent of eye development completely followed our *a priori* prediction of *Pax6* activity.

Mouse and human *Pax6* allele databases: *PAX6/Pax6* functions as a transcription factor via DNA binding of its binding domains to different target genes and mutations affecting different specific regions of the *Pax6* gene product may result in different aberrant phenotypes (Tang *et al.* 1997; Singh *et al.* 2000; Haubst *et al.* 2004). There is an extensive human *PAX6* allelic variant database (http://pax6.hgu.mrc.ac.uk) last updated September 27, 2007, with 408 entries. Most *PAX6* mutations result in premature termination of the translation product and there were 61 missense mutations: 43 in the paired domain, one in the linker region, 5 in the homeodomain, 12 in the P/S/T region, 4 at the Met start codon, and 15 at the stop codon. Genotype–phenotype correlations have shown that mutations resulting in premature termination of the translation of the *PAX6* gene product are mostly associated with aniridia, while missense mutations are often associated with nonaniridia phenotypes (Azuma *et al.* 1996, 1998, 1999; Azuma and Yamada 1998; Tzoulaki *et al.* 2005). The mouse mutant-allele database (http://www.informatics.jax.org) contains 32 entries. Twenty-four mutant alleles were recovered in phenotype screens and eight entries represent mutant knockout or conditional knockout constructs. Of the 24 mutant alleles recovered in phenotype-based screens, most result in premature truncation of the translation product or deletions of the *Pax6* gene. Two *Pax6* alleles are missense mutations in the paired domain, $Pax6^{Leca2}$ and $Pax6^{Leca4}$ (Thaung *et al.* 2002) and four missense mutations have been identified in the homeodomain, $Pax6^{4Neu}$ (Favor *et al.* 2001), $Pax6^{Leca1}$ (Thaung *et al.* 2002), $Pax6^{1Jrt}$ (Rossant 2003), and $Pax6^{132\text{-}14Neu}$ (this study). It is interesting to note that all missense mutations in the mouse in the homeodomain are at amino acid sites within the third helix of the homeodomain.

General conclusions: An extensive allelic series is useful for genetic, molecular, and development analyses of gene function. Detailed *in vivo* analyses are usually possible only in model laboratory organisms. This study has extended the mouse allelic series of the *Pax6* gene to include a homozygous and hemizygous viable and fertile hypomorph allele. In our genotype–phenotype studies to correlate levels of *Pax6* activity with the degree of aberrant development, we have focused on the eye. Obviously, similar studies with other organs in which *Pax6* plays an important role in development would be interesting. For example, the mechanisms leading to lethality of *Pax6* mutant neonates is still not known. The best candidates are neurologic or metabolic dysfunctions due to the brain and the pancreas developmental defects. Here, analyses of brain or pancreas development in the *Pax6* mutant genotype constructs could be informative.

We thank Laure Bally-Cuif and Magdalena Götz for critically reading our manuscript, and we greatly appreciate the expert technical assistance of Oceane Anezo, Sibylle Frischholz, Bianca Hildebrand, Brigitta May, and Sylvia Wolf. Research was partially supported by National Institutes of Health grant R0-1EY10321.

LITERATURE CITED

Ashery-Padan, R., T. Marquardt, X. Zhou and P. Gruss, 2000 Pax6 activity in the lens primordium is required for lens

formation and for correct placement of a single retina in the eye. Genes Dev. **14:** 2701–2711.

Azuma, N., and M. Yamada, 1998 Missense mutation at the C terminus of the *PAX6* gene in ocular anterior segment anomalies. Invest. Ophthalmol. Vis. Sci. **39:** 828–830.

Azuma, N., S. Nishina, H. Yanagisawa, T. Okuyama and M. Yamada, 1996 *PAX6* missense mutation in isolated foveal hypoplasia. Nat. Genet. **13:** 141–142.

Azuma, N., Y. Hotta, H. Tanaka and M. Yamada, 1998 Missense mutations in the *PAX6* gene in aniridia. Invest. Ophthalmol. Vis. Sci. **39:** 2524–2528.

Azuma, N., Y. Yamaguchi, H. Handa, M. Hayakawa, A. Kanai *et al.*, 1999 Missense mutation in the alternative splice region of the PAX6 gene in eye anomalies. Am. J. Hum. Genet. **65:** 656–663.

Baulmann, D. C., A. Ohlmann, C. Flügel-Koch, S. Goswami, A. Cvekl *et al.*, 2002 *Pax6* heterozygous eyes show defects in chamber angle differentiation that are associated with a wide spectrum of other anterior eye segment abnormalities. Mech. Dev. **118:** 3–17.

Bentley, C. A., M. P. Zidehsarai, J. C. Grindley, A. F. Parlow, S. Barth-Hall *et al.*, 1999 *Pax6* is implicated in murine pituitary endocrine function. Endocrine **10:** 171–177.

Bruun, J. A., E. I. Thomassen, K. Kristiansen, G. Tylden, T. Holm *et al.*, 2005 The third helix of the homeodomain of paired class homeodomain proteins acts as a recognition helix both for DNA and protein interactions. Nucleic Acids Res. **33:** 2661–2675.

Canto-Soler, M. V., and R. Adler, 2006 Optic cup and lens development requires Pax6 expression in the early optic vesicle during a narrow time window. Dev. Biol. **294:** 119–132.

Carrière, C., S. Plaza, P. Martin, B. Quatannens, M. Bailly *et al.*, 1993 Characterization of quail Pax-6 (Pax-QNR) proteins expressed in the neuroretina. Mol. Cell. Biol. **13:** 7257–7266.

Carrière, C., S. Plaza, J. Caboche, C. Dozier, M. Bailly *et al.*, 1995 Nuclear localization signals, DNA binding, and transactivation properties of quail *Pax-6* (*Pax-QNR*) isoforms. Cell Growth Differ. **6:** 1531–1540.

Chi, N., and J. A. Epstein, 2002 Getting your Pax straight: Pax proteins in development and disease. Trends Genet. **18:** 41–47.

Collinson, J. M., R. E. Hill and J. D. West, 2000 Different roles for *Pax6* in the optic vesicle and facial epithelium mediate early morphogenesis of the murine eye. Development **127:** 945–956.

Collinson, J. M., J. C. Quinn, M. A. Buchanan, M. H. Kaufman, S. E. Wedden *et al.*, 2001 Primary defects in the lens underlie complex anterior segment abnormalities of the *Pax6* heterozygous eye. Proc. Natl. Acad. Sci. USA **98:** 9688–9693.

Collinson, J. M., J. C. Quinn, R. E. Hill and J. D. West, 2003 The roles of *Pax6* in the cornea, retina, and olfactory epithelium of the developing mouse embryo. Dev. Biol. **255:** 303–312.

Czerny, T., and M. Busslinger, 1995 DNA-binding and transactivation properties of Pax-6: three amino acids in the paired domain are responsible for the different sequence recognition of Pax-6 and BSAP (Pax-5). Mol. Cell. Biol. **15:** 2858–2871.

Davis-Silberman, N., T. Kalich, V. Oron-Karni, T. Marquardt, M. Kroeber *et al.*, 2005 Genetic dissection of Pax6 dosage requirements in the developing mouse eye. Hum. Mol. Genet. **14:** 2265–2276.

Duncan, M. K., Z. Kozmik, K. Cveklova, J. Piatigorsky and A. Cvekl, 2000 Overexpression of PAX6(5a) in lens fiber cells results in cataract and upregulation of α5β1 integrin expression. J. Cell Sci. **113:** 3173–3185.

Estivill-Torrús, G., T. Vitalis, P. Fernández-Llebrez and D. J. Price, 2001 The transcription factor Pax6 is required for development of the diencephalic dorsal midline secretory radial glia that form the subcommissural organ. Mech. Dev. **109:** 215–224.

Favor, J., 1983 A comparison of the dominant cataract and recessive specific-locus mutation rates induced by treatment of male mice with ethylnitrosourea. Mutat. Res. **110:** 367–382.

Favor, J., P. Grimes, A. Neuhäuser-Klaus, W. Pretsch and D. Stambolian, 1997 The mouse *Cat4* locus maps to chromosome 8 and mutants express lens-corneal adhesion. Mamm. Genome **8:** 403–406.

Favor, J., H. Peters, T. Hermann, W. Schmahl, B. Chatterjee *et al.*, 2001 Molecular characterization of *Pax6*^{2Neu} through *Pax6*^{10Neu}: an extension of the *Pax6* allelic series and the identification of two possible hypomorph alleles in the mouse *Mus musculus*. Genetics **159:** 1689–1700.

Favor, J., C. J. Gloeckner, D. Janik, M. Klempt, A. Neuhäuser-Klaus *et al.*, 2007 Type IV procollagen missense mutations associated with defects of the eye, vascular stability, the brain, kidney function and embryonic or postnatal viability in the mouse, *Mus musculus*: an extension of the *Col4a1* allelic series and the identification of the first two *Col4a2* mutant alleles. Genetics **175:** 725–736.

Gehring, W. J., Y. Q. Qian, M. Billeter, K. Furukubo-Tokunaga, A. F. Schier *et al.*, 1994 Homeodomain-DNA recognition. Cell **78:** 211–223.

Glaser, T., L. Jepeal, J. G. Edwards, S. R. Young, J. Favor *et al.*, 1994 PAX6 gene dosage effect in a family with congenital cataracts, aniridia, anophthalmia and central nervous system defects. Nat. Genet. **7:** 463–471.

Gorlov, I. P., and G. F. Saunders, 2002 A method for isolating alternatively spliced isoforms: isolation of murine *Pax6* isoforms. Anal. Biochem. **308:** 401–404.

Götz, M., A. Stoykova and P. Gruss, 1998 *Pax6* controls radial glia differentiation in the cerebral cortex. Neuron **21:** 1031–1044.

Grindley, J. C., D. R. Davidson and R. E. Hill, 1995 The role of *Pax-6* in eye and nasal development. Development **121:** 1433–1442.

Grindley, J. C., L. K. Hargett, R. E. Hill, A. Ross and B. L. Hogan, 1997 Disruption of PAX6 function in mice homozygous for the *Pax6*$^{Sey\text{-}1Neu}$ mutation produces abnormalities in the early development and regionalization of the diencephalon. Mech. Dev. **64:** 111–126.

Hack, M. A., A. Saghatelyan, A. de Chevigny, A. Pfeifer, R. Ashery-Padan *et al.*, 2005 Neuronal fate determinants of adult olfactory bulb neurogenesis. Nat. Neurosci. **8:** 865–872.

Hanes, S. D., and R. Brent, 1989 DNA specificity of the bicoid activator protein is determined by homeodomain recognition helix residue 9. Cell **57:** 1275–1283.

Haubst, N., J. Berger, V. Radjendirane, J. Graw, J. Favor *et al.*, 2004 Molecular dissection of Pax6 function: the specific roles of the paired domain and homeodomain in brain development. Development **131:** 6131–6140.

Heins, N., P. Malatesta, F. Cecconi, M. Nakafuku, K. L. Tucker *et al.*, 2002 Glial cells generate neurons: the role of the transcription factor Pax6. Nat. Neurosci. **5:** 308–315.

Heinzmann, U., J. Favor, J. Plendl and G. Grevers, 1991 Entwicklungsstörung des olfaktorischen Organs. Ein Beitrag zur kausalen Genese bei einer Mausmutante. Verh. Anat. Ges. **85:** 511–512.

Hill, R. E., J. Favor, B. L. Hogan, C. C. Ton, G. F. Saunders *et al.*, 1991 Mouse *Small eye* results from mutations in a paired-like homeobox-containing gene. Nature **354:** 522–525.

Hogan, B. L., G. Horsburgh, J. Cohen, C. M. Hetherington, G. Fisher *et al.*, 1986 *Small eyes* (*Sey*): a homozygous lethal mutation on chromosome 2 which affects the differentiation of both lens and nasal placodes in the mouse. J. Embryol. Exp. Morphol. **97:** 95–110.

Hogan, B. L., E. M. Hirst, G. Horsburgh and C. M. Hetherington, 1988 *Small eye* (*Sey*): a mouse model for the genetic analysis of craniofacial abnormalities. Development **103**(Suppl): 115–119.

Kaufman, M. H., H. H. Chang and J. P. Shaw, 1995 Craniofacial abnormalities in homozygous *Small eye* (*Sey/Sey*) embryos and newborn mice. J. Anat. **186**(Pt 3): 607–617.

Kim, J., and J. D. Lauderdale, 2006 Analysis of Pax6 expression using a BAC transgene reveals the presence of a paired-less isoform of Pax6 in the eye and olfactory bulb. Dev. Biol. **292:** 486–505.

Kim, J., and J. D. Lauderdale, 2008 Overexpression of pairedless Pax6 in the retina disrupts corneal development and affects lens cell survival. Dev. Biol. **313:** 434–454.

Kioussi, C., S. O'Connell, L. St-Onge, M. Treier, A. S. Gleiberman *et al.*, 1999 *Pax6* is essential for establishing ventral-dorsal cell boundaries in pituitary gland development. Proc. Natl. Acad. Sci. USA **96:** 14378–14382.

Kratochvilova, J., and U. H. Ehling, 1979 Dominant cataract mutations induced by gamma-irradiation of male mice. Mutat. Res. **63:** 221–223.

Kratochvilova, J., and J. Favor, 1992 Allelism tests of 15 dominant cataract mutations in mice. Genet. Res. **59:** 199–203.

Li, H. S., J. M. Yang, R. D. Jacobson, D. Pasko and O. Sundin, 1994 Pax-6 is first expressed in a region of ectoderm anterior

to the early neural plate: implications for stepwise determination of the lens. Dev. Biol. **162:** 181–194.

Lyon, M. F., D. Bogani, Y. Boyd, P. Guillot and J. Favor, 2000 Further genetic analysis of two autosomal dominant mouse eye defects, *Ccw* and *Pax6*^{coop}. Mol. Vis. **6:** 199–203.

Manly, K. F., 1993 A Macintosh program for storage and analysis of experimental genetic mapping data. Mamm. Genome **4:** 303–313.

Manuel, M., P. A. Georgala, C. B. Carr, S. Chanas, D. A. Kleinjan *et al.*, 2007 Controlled overexpression of Pax6 in vivo negatively autoregulates the *Pax6* locus, causing cell-autonomous defects of late cortical progenitor proliferation with little effect on cortical arealization. Development **134:** 545–555.

Mishra, R., I. P. Gorlov, L. Y. Chao, S. Singh and G. F. Saunders, 2002 PAX6, paired domain influences sequence recognition by the homeodomain. J. Biol. Chem. **277:** 49488–49494.

Planque, N., L. Leconte, F. M. Coquelle, S. Benkhelifa, P. Martin *et al.*, 2001 Interaction of Maf transcription factors with Pax-6 results in synergistic activation of the glucagon promoter. J. Biol. Chem. **276:** 35751–35760.

Plaza, S., S. Saule and C. Dozier, 1999 High conservation of cis-regulatory elements between quail and human for the *Pax-6* gene. Dev. Genes Evol. **209:** 165–173.

Qian, Y. Q., D. Resendez-Perez, W. J. Gehring and K. Wüthrich, 1994 The des(1-6)antennapedia homeodomain: comparison of the NMR solution structure and the DNA-binding affinity with the intact Antennapedia homeodomain. Proc. Natl. Acad. Sci. USA **91:** 4091–4095.

Quinn, J. C., J. D. West and R. E. Hill, 1996 Multiple functions for *Pax6* in mouse eye and nasal development. Genes Dev. **10:** 435–446.

Ritz-Laser, B., A. Estreicher, N. Klages, S. Saule and J. Philippe, 1999 Pax-6 and Cdx-2/3 interact to activate glucagon gene expression on the G1 control element. J. Biol. Chem. **274:** 4124–4132.

Rossant, J., 2003 A new allele at the Pax6 locus from the Center of Modelling Human Disease. Mouse Genome Database. http://www.informatics.jax.org.

Schedl, A., A. Ross, M. Lee, D. Engelkamp, P. Rashbass *et al.*, 1996 Influence of *PAX6* gene dosage on development: overexpression causes severe eye abnormalities. Cell **86:** 71–82.

Schmahl, W., M. Knoedlseder, J. Favor and D. Davidson, 1993 Defects of neuronal migration and the pathogenesis of cortical malformations are associated with Small eye (Sey) in the mouse, a point mutation at the Pax-6-locus. Acta Neuropathol. **86:** 126–135.

Singh, S., C. M. Stellrecht, H. K. Tang and G. F. Saunders, 2000 Modulation of PAX6 homeodomain function by the paired domain. J. Biol. Chem. **275:** 17306–17313.

Singh, S., L. Y. Chao, R. Mishra, J. Davies and G. F. Saunders, 2001 Missense mutation at the C-terminus of PAX6 negatively modulates homeodomain function. Hum. Mol. Genet. **10:** 911–918.

St-Onge, L., B. Sosa-Pineda, K. Chowdhury, A. Mansouri and P. Gruss, 1997 *Pax6* is required for differentiation of glucagon-producing alpha-cells in mouse pancreas. Nature **387:** 406–409.

Stoykova, A., R. Fritsch, C. Walther and P. Gruss, 1996 Forebrain patterning defects in *Small eye* mutant mice. Development **122:** 3453–3465.

Stoykova, A., M. Götz, P. Gruss and J. Price, 1997 *Pax6*-dependent regulation of adhesive patterning, R-cadherin expression and boundary formation in developing forebrain. Development **124:** 3765–3777.

Stoykova, A., D. Treichel, M. Hallonet and P. Gruss, 2000 *Pax6* modulates the dorsoventral patterning of the mammalian telencephalon. J. Neurosci. **20:** 8042–8050.

Talamillo, A., J. C. Quinn, J. M. Collinson, D. Caric, D. J. Price *et al.*, 2003 *Pax6* regulates regional development and neuronal migration in the cerebral cortex. Dev. Biol. **255:** 151–163.

Tang, H. K., L. Y. Chao and G. F. Saunders, 1997 Functional analysis of paired box missense mutations in the *PAX6* gene. Hum. Mol. Genet. **6:** 381–386.

Thaung, C., K. West, B. J. Clark, L. McKie, J. E. Morgan *et al.*, 2002 Novel ENU-induced eye mutations in the mouse: models for human eye disease. Hum. Mol. Genet. **11:** 755–767.

Theiler, K., D. S. Varnum and L. C. Stevens, 1978 Development of Dickie's small eye, a mutation in the house mouse. Anat. Embryol. **155:** 81–86.

Ton, C. C., H. Hirvonen, H. Miwa, M. M. Weil, P. Monaghan *et al.*, 1991 Positional cloning and characterization of a paired box- and homeobox-containing gene from the aniridia region. Cell **67:** 1059–1074.

Treisman, J., P. Gönczy, M. Vashishtha, E. Harris and C. Desplan, 1989 A single amino acid can determine the DNA binding specificity of homeodomain proteins. Cell **59:** 553–562.

Tzoulaki, I., I. M. White and I. M. Hanson, 2005 *PAX6* mutations: genotype-phenotype correlations. BMC Genet. **6:** 27.

van Raamsdonk, C. D., and S. M. Tilghman, 2000 Dosage requirement and allelic expression of *PAX6* during lens placode formation. Development **127:** 5439–5448.

Walther, C., and P. Gruss, 1991 *Pax-6*, a murine paired box gene, is expressed in the developing CNS. Development **113:** 1435–1450.

Wawersik, S., P. Purcell and R. L. Maas, 2000 *Pax6* and the genetic control of early eye development. Results Probl. Cell. Differ. **31:** 15–36.

Wilson, D., G. Sheng, T. Lecuit, N. Dostatni and C. Desplan, 1993 Cooperative dimerization of paired class homeo domains on DNA. Genes Dev. **7:** 2120–2134.

Communicating editor: T. R. Magnuson